

# Synthesis and Application of $\text{Fe}_3\text{O}_4@Au$ Composite Nanoparticles as Magnetic Resonance/Computed Tomography Dual-Modality Contrast Agent

## Abstract

**Background:** None of the molecular imaging modalities can produce imaging with both anatomical and functional information. In recent years, to overcome these limitations multimodality molecular imaging or combination of two imaging modalities can provide anatomical and pathological information. **Methods:** Magnetic iron oxide nanoparticles were prepared by co-precipitation method and then were coated with silica according to Stober method. Consequently, silica-coated nanoparticles were amino-functionalized. Finally, gold nanoparticles assembled onto the surfaces of the previous product. Cytotoxicity effects of prepared  $\text{Fe}_3\text{O}_4@Au$  nanoparticles were evaluated by 3-(4,5-dimethylthiazol-2-yl)-2,5-diphenyltetrazolium bromide assay on human hepatocellular carcinoma cells. Their ability as a dual-mode contrast agent was investigated by magnetic resonance (MR) and computed tomography (CT) imaging. **Results:**  $\text{Fe}_3\text{O}_4@Au$  nanoparticles were spherical undersize of 75 nm. X-ray diffraction analysis confirmed the formation of  $\text{Fe}_3\text{O}_4@Au$  nanoparticles. The magnetometry result confirmed the superparamagnetism property of prepared nanoparticles, and the saturation magnetization ( $M_s$ ) was found to be 33 emu/g.  $\text{Fe}_3\text{O}_4@Au$  nanoparticles showed good cytocompatibility up to 60  $\mu\text{g}/\text{mL}$ . The results showed that the  $\text{Fe}_3\text{O}_4@Au$  nanoparticles have good  $r_2$  relaxivity ( $135.26 \text{ mM}^{-1}\text{s}^{-1}$ ) and good X-ray attenuation property. **Conclusion:** These findings represent that prepared  $\text{Fe}_3\text{O}_4@Au$  nanoparticles in an easy and relatively low-cost manner have promising potential as a novel contrast agent for dual-modality of MR/CT imaging.

**Keywords:** *Computed tomography, gold nanoparticles, iron oxide nanoparticles, magnetic resonance imaging*

Submitted: 19-Oct-2019

Revision: 13-Dec-2019

Accepted: 30-Dec-2019

Published: 03-Jul-2020

## Introduction

Molecular imaging can be defined as the imaging of targeted macromolecules and biological processes in living organisms.<sup>[1,2]</sup> Recently, it has gained great attention in biomedical sciences. Based on the molecular imaging, molecular profiles and/or cell behavior altered prior to these alteration can be visualized anatomically. Thereby, this had predisposed molecular imaging to early detection of disease with high sensitivity and specificity.<sup>[1,3]</sup>

Nanoparticles have gained great attention for applications in medicine, including cancer treatment and molecular imaging.<sup>[4,5]</sup> There are different methods of molecular imaging, including magnetic resonance imaging (MRI),<sup>[6]</sup> computed tomography (CT),<sup>[7]</sup> ultrasound, and nuclear

medicine modalities.<sup>[8-10]</sup> The important point is that each modality has limitations and advantages over each other, that is, none of them is able to completely give anatomical and pathological data independently.<sup>[11]</sup> Therefore, it can be useful to combine two or more imaging modalities.

Among them, MRI is a noninvasive and nonionizing type of radiation with high spatial resolution and superior soft-tissue contrast.<sup>[12,13]</sup> Meanwhile, CT imaging has a high resolution, three-dimensional tomography technique, so that its density resolution is better than alternative imaging modalities.<sup>[14]</sup> Therefore, combining CT and MRI can help to accurate disease diagnosis.

Nanoparticles have gained great attention for applications in molecular imaging. In recent decades, superparamagnetic

This is an open access journal, and articles are distributed under the terms of the Creative Commons Attribution-NonCommercial-ShareAlike 4.0 License, which allows others to remix, tweak, and build upon the work non-commercially, as long as appropriate credit is given and the new creations are licensed under the identical terms.

For reprints contact: [reprints@medknow.com](mailto:reprints@medknow.com)

**How to cite this article:** Keshtkar M, Shahbazi-Gahrouei D, Mahmoudabadi A. Synthesis and application of  $\text{Fe}_3\text{O}_4@Au$  composite nanoparticles as magnetic resonance/computed tomography dual-modality contrast agent. *J Med Signals Sens* 2020;10:201-7.

Mohammad Keshtkar<sup>1</sup>,  
Daryoush Shahbazi-Gahrouei<sup>2</sup>,  
Alireza Mahmoudabadi<sup>1</sup>

<sup>1</sup>Department of Medical Physics and Radiology, Gonabad University of Medical Sciences, Gonabad, <sup>2</sup>Department of Medical Physics, Isfahan University of Medical Sciences, Isfahan, Iran

**Address for correspondence:**  
Dr. Mohammad Keshtkar,  
Department of Medical Physics and Radiology,  
Gonabad University of Medical Sciences, Gonabad, Iran.  
E-mail: [keshtkar.dmohammad@yahoo.com](mailto:keshtkar.dmohammad@yahoo.com)

Access this article online

Website: [www.jmssjournal.net](http://www.jmssjournal.net)

DOI: 10.4103/jmss.JMSS\_55\_19

Quick Response Code:



iron oxide nanoparticles have been typically utilized as T<sub>2</sub>-weighted MRI contrast agent due to their capability to dephase transverse magnetization and thereby reducing T<sub>2</sub> relaxation times of water protons.<sup>[15]</sup> Nanoparticles with high X-ray absorption can be utilized as a contrast agent for CT imaging. For example, gold nanoparticles due to their higher X-ray absorption coefficient and good biocompatibility have been widely applied for CT imaging.<sup>[16]</sup> Therefore, combination of Fe<sub>3</sub>O<sub>4</sub> and Au nanoparticles have been applied for MRI/CT dual-modality imaging.<sup>[17]</sup>

There are some studies about synthesizing and application of different nanocomposites with different construction method in dual-modal imaging, such as polyethylenimine (PEI)-entrapped gold nanoparticles chelated with gadolinium (Gd) ions,<sup>[18]</sup> TbF<sub>3</sub>,<sup>[19]</sup> GdF<sub>3</sub>,<sup>[20]</sup> strawberry-like Fe<sub>3</sub>O<sub>4</sub>-Au nanoparticles,<sup>[21]</sup> gadolinium-loaded dendrimer-entrapped gold nanoparticles,<sup>[22]</sup> PEI-Au-Gd nanoparticles,<sup>[23]</sup> Fe<sub>2</sub>O<sub>3</sub>@Au nanoparticles,<sup>[24]</sup> FePt,<sup>[25]</sup> and Fe<sub>3</sub>O<sub>4</sub>/Au.<sup>[26]</sup>

It has been proved that Fe<sub>3</sub>O<sub>4</sub> nanoparticles can improve image contrast and sensitivity in MRI.<sup>[26]</sup> Furthermore, gold improves CT image contrast in nanoparticle format.<sup>[22]</sup> Yu *et al.*<sup>[27]</sup> and Hu *et al.*<sup>[11]</sup> developed dumbbell-like Au-Fe<sub>3</sub>O<sub>4</sub> nanocomposites in heating condition of approximately 300°C and Fe<sub>3</sub>O<sub>4</sub>/Au nanocomposites at 80°C, respectively. He *et al.* developed Fe<sub>2</sub>O<sub>3</sub>@Au nanoparticles by oxidizing Fe<sub>3</sub>O<sub>4</sub> seed using HNO<sub>3</sub> solution with stirring at 100°C.<sup>[24]</sup> Cai *et al.* reported developing Fe<sub>3</sub>O<sub>4</sub>/Au nanocomposites in relatively high cost, complicated and time-consuming manner with layer by layer self-assembly technique and iterative Au salt reduction process.<sup>[26]</sup> In the synthesizing process, it is desirable to develop nanocomposites in relatively easy manner, using low-cost materials and in-room temperature; therefore, the main goal of this manuscript is to evaluate new developed nanocomposite structure for magnetic resonance (MR)/CT imaging.

## Materials and Methods

### Materials

Ferrous chloride tetrahydrate (FeCl<sub>2</sub>·4H<sub>2</sub>O, >99%), ferric chloride hexahydrate (FeCl<sub>3</sub>·6H<sub>2</sub>O) (>99%), hydrochloric acid (HCl, 37%), Si(OC<sub>2</sub>H<sub>5</sub>)<sub>4</sub> (tetraethyl orthosilicate [TEOS]), ammonia aqueous (25 wt%), and ethanol and toluene (>99%) were purchased from Merck. Sodium borohydride (NaBH<sub>4</sub>), 3-aminopropyltriethoxysilane (APTES), and chloroauric acid (HAuCl<sub>4</sub>) were obtained from Sigma (St. Louis, MO, USA). Deionized water was used throughout the experiment.

### Synthesis of Fe<sub>3</sub>O<sub>4</sub>@Au nanoparticles

Chemical co-precipitation of Fe<sup>2+</sup> and Fe<sup>3+</sup> salts by the addition of a base in aqueous media was used for Fe<sub>3</sub>O<sub>4</sub> synthesis.<sup>[28]</sup> First, FeCl<sub>3</sub>·6H<sub>2</sub>O, and FeCl<sub>2</sub>·4H<sub>2</sub>O with

certain molar ratio were dissolved in 40 ml HCl (0.4 M). Then, a 400 mL NH<sub>3</sub> solution was quickly added under vigorous stirring. After precipitation, Fe<sub>3</sub>O<sub>4</sub> nanoparticles magnetically collected, repeatedly washed, and re-dispersed in 150 mL of deionized water.

Fe<sub>3</sub>O<sub>4</sub> nanoparticles were coated with the SiO<sub>2</sub> by modifying Stober method.<sup>[29]</sup> Briefly, 30 mL suspension of Fe<sub>3</sub>O<sub>4</sub> nanoparticles, 15 mL ammonia, 30 mL water, and 1.9 mL TEOS were added into 300 mL 2-propanol under vigorous stirring for 18 h. Finally, Fe<sub>3</sub>O<sub>4</sub>@SiO<sub>2</sub> was collected by magnet separation and washed several times.

In the next step, the previous product was amino-functionalization by APTES. Briefly, 6 gr Fe<sub>3</sub>O<sub>4</sub>@SiO<sub>2</sub> and 16 mL APTES were added into 60 mL anhydrous toluene with stirring overnight while the solution was deoxygenized by the argon. The Fe<sub>3</sub>O<sub>4</sub>@SiO<sub>2</sub>/NH<sub>2</sub> washed with acetone and finally dried under vacuum.

In the final stage, 30 mg Fe<sub>3</sub>O<sub>4</sub>@SiO<sub>2</sub>/NH<sub>2</sub> was dispersed in 45 mL water at pH = 4 under ultrasonication for 60 min. Subsequently, 15 mL HAuCl<sub>4</sub> aqueous solution (1.71 mM) was added to the MNPs. At the end, 15 mL NaBH<sub>4</sub> solution (0.1 M) was added to the mixture. Finally, the product was collected and washed using phosphate-buffered saline (PBS) (pH = 7.4).

### Characterization

Transmission electron microscopy images were recorded on a Philips-EM208S at an accelerating voltage of 100 kV. Fourier transform infrared (FTIR) spectroscopy study was carried out by JASCO, FT/IR-6300 (Japan), to determine the chemical functional groups in the nanoparticles at various steps of synthesis. The magnetic properties of nanoparticles were evaluated by the Alternating Gradient Field Magnetometry at room temperature up to 9000 Oe. X-ray diffraction (XRD) study was through a Bruker X-ray diffractometer. The iron and gold concentrations of the stock solution were measured using an atomic absorption spectrophotometer (Shimadzu, AA-680).

### Cell culture

The human hepatocellular carcinoma (HepG2) cells were grown in RPMI-1640 medium supplemented with 10% fetal bovine serum, penicillin (100 U/mL), and streptomycin (100 µg/mL). The cells were maintained at 37°C in a humidified incubator with 5% CO<sub>2</sub>.<sup>[30]</sup>

### Cytotoxicity assay

*In vitro* cytotoxicity of the Fe<sub>3</sub>O<sub>4</sub>@Au nanoparticles was evaluated by 3-(4,5-dimethylthiazol-2-yl)-2,5-diphenyltetrazolium bromide (MTT) assay on HepG2 cells. Briefly, HepG2 cells were grown into 96-well cell plates at a density of 5,000 cells per well and incubated overnight in a humidified incubator with a CO<sub>2</sub> concentration of 5%. Then, the cells

were incubated with various concentrations of Fe<sub>3</sub>O<sub>4</sub>@Au nanoparticles ranging from 10 to 80 µg/mL for 24 h. A culture medium without any nanoparticles prepared as the control wells.

Thereafter, MTT (20 µL in PBS, 5 mg/mL) was added to each well and further incubated for 4 h. Then, the culture medium was carefully removed, and 200 µL DMSO was added to each well to dissolve insoluble Formazan crystals. The absorbance at 570 nm in each well was recorded using an ELISA reader (Synergy H1, Bio Tek). Mean and standard deviation of three wells were expressed for each sample. The percentage of cell viability was measured by dividing viable cells in each well by control wells.

### T<sub>2</sub> relaxivity measurement and X-ray attenuation property

The efficiency of an MRI contrast agent is determined by its ability to manipulate relaxation rates.<sup>[31]</sup> Due to MRI contrast agents change the T<sub>1</sub> and T<sub>2</sub> relaxation times of the abundant water, the relaxivity of a contrast agent is presented by its change in the water proton relaxation times.<sup>[32]</sup> In the case of T<sub>2</sub>-weighted contrast agent, transverse relaxation rates are altered in the existence of a contrast agent by

$$R_2 = 1/T_2 + r_2 C. [32]$$

Where C is its concentration, and r<sub>2</sub> is transverse relaxivity. Moreover, in the absence of contrast agents, C = 0, R<sub>2</sub> is unperturbed water transverse relaxation rate.

For determining relaxivity, solutions of Fe<sub>3</sub>O<sub>4</sub>@Au nanoparticles were prepared in water at different iron concentrations. MRI was performed at room temperature using a 1.5 T scanner (Symphony, Siemens). T<sub>2</sub> relaxivity was determined using multiple spin-echo sequences utilizing 16 echo-times ranging from 22 to 352 ms and a repetition time of 3000 ms.<sup>[33]</sup> The other parameters were set as follow: slice thickness = 3 mm, number of excitation = 1, acquisition matrix = 128 × 128. T<sub>2</sub> relaxivity (r<sub>2</sub> in mM<sup>-1</sup>s<sup>-1</sup>) was calculated from the slopes of 1/T<sub>2</sub> against Fe concentration.

Evaluating the ability of the Fe<sub>3</sub>O<sub>4</sub>@Au nanoparticles in attenuating X-ray was performed using a clinical 64 slice scanner (SOMATOM sensation, Siemens) with 80 kV, 300 mAs, and a slice thickness of 0.6 mm. The samples prepared in water with various Au concentrations were put into 2 mL Eppendorf tubes. The assessment of nanoparticles in X-ray attenuation was performed by importing the CT images in ImageJ program and then drawing a region of interest in CT image for each sample.

## Results

### Nanoparticles characterization

The size of the Fe<sub>3</sub>O<sub>4</sub>@Au nanoparticles was revealed by TEM imaging. The obtained Fe<sub>3</sub>O<sub>4</sub>@Au nanoparticles had a spherical morphology with a size of <75 nm [Figure 1].

The structure of the synthesized Fe<sub>3</sub>O<sub>4</sub>@Au nanoparticles was characterized by XRD [Figure 2]. Theta is the angle between incident and reflected ray. The diffraction peaks observed at 30.3° (220), 35.6° (311), 43.2° (400), 53.4° (422), 57.2° (511), 62.7° (440) could be assigned to Fe<sub>3</sub>O<sub>4</sub>. Furthermore, the peaks observed at 38.2°, 44.4°, 64.5°, and 77.4° could be related to the reflections of the (111), (200), (220), and (311) crystalline planes of cubic Au, respectively.

The chemical composition of the obtained nanoparticles was analyzed by FTIR spectrum as shown in Figure 3. The absorption peaks at 3417 are associated with the N–H stretching vibration. Furthermore, the presence of the propyl groups in APTES molecules is revealed by C–H stretching vibrations that emerged at 2930 and 2862 cm<sup>-1</sup>. It should be noted that there is no absorption band for the Au in the infrared region.

Figure 4 shows the magnetic hysteresis loop of Fe<sub>3</sub>O<sub>4</sub>@Au nanoparticles at room temperature. In fact, it represents the plot of the magnetization “M” versus the applied field “H” (between –9 and +9 kOe) of the synthesized Fe<sub>3</sub>O<sub>4</sub>@Au nanoparticles. The saturation magnetization (M<sub>s</sub>) was around 33 emu/g.

### Cytotoxic assay

The biocompatibility of the nanoparticles was assessed on HepG2 cells by MTT assay. Figure 5 showed the result of MTT assay at different concentrations. The results are presented in terms of percentage cell viability. Materials with cell viability above 80% can be accepted as biocompatible material.<sup>[34]</sup> Findings showed that for HepG2 cells, at concentration of 80 µg/mL Fe<sub>3</sub>O<sub>4</sub>@Au nanoparticles have cytotoxicity effects. Indeed, at concentrations from 10 up to 60 µg/mL cell toxicity is low or moderate.

### T<sub>2</sub> relaxivity measurement and X-ray attenuation property

The role of Fe<sub>3</sub>O<sub>4</sub> nanoparticles as an MRI contrast agent is to decrease transverse relaxation time. T<sub>2</sub>-weighted MR

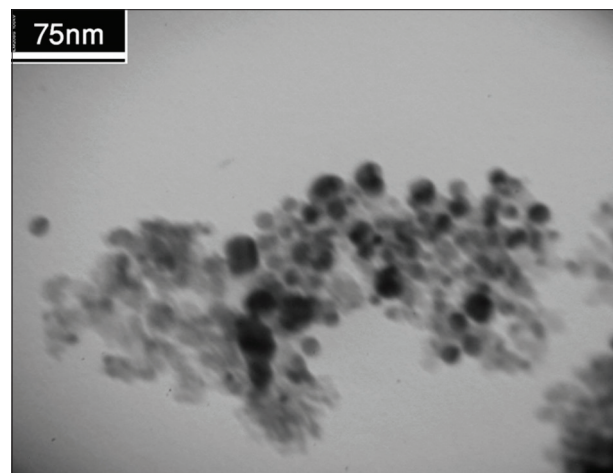


Figure 1: Transmission electron microscopy image of prepared Fe<sub>3</sub>O<sub>4</sub>@Au nanoparticles

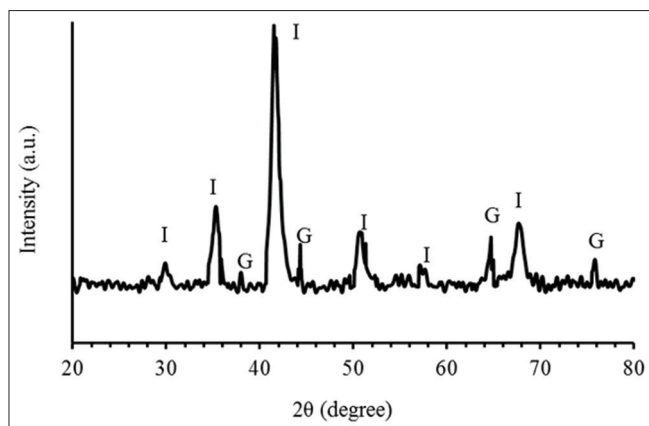


Figure 2: X-ray diffraction pattern of the formed Fe<sub>3</sub>O<sub>4</sub>@Au nanoparticles ("I" and "G" for Fe<sub>3</sub>O<sub>4</sub> and Au nanoparticles, respectively)

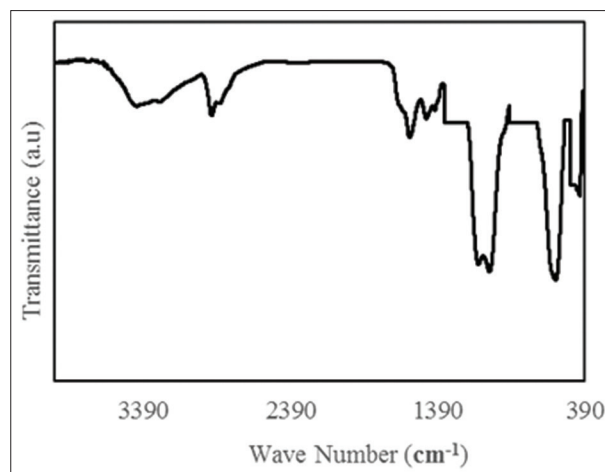


Figure 3: Fourier transform infrared spectrum of Fe<sub>3</sub>O<sub>4</sub>@Au nanoparticles

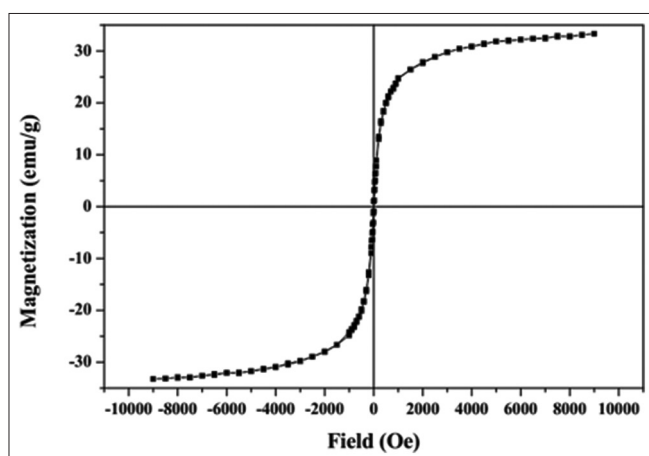


Figure 4: Magnetization curve of Fe<sub>3</sub>O<sub>4</sub>@Au nanoparticles

relaxometry of the Fe<sub>3</sub>O<sub>4</sub>@Au nanoparticles was performed to confirm their application as a contrast agent for MRI [Figure 6a]. Transverse relaxivity ( $r_2$ ) was measured by plotting  $1/T_2$  against the iron concentration in the solution [Figure 6b]. The measured relaxivity, which is the slope of the plot was  $135.26 \text{ mM}^{-1}\text{s}^{-1}$ .

X-ray attenuation property of Fe<sub>3</sub>O<sub>4</sub>@Au nanoparticles was investigated to confirm their use as CT contrast agent. Figure 7 shows the CT image of nanoparticles with different Au concentrations (a) and the plot of the Hounsfield units against Au concentration (b). As the Au concentration increases, the CT image intensity increases.

## Discussion

Figure 1 shows the TEM image of Fe<sub>3</sub>O<sub>4</sub>@Au nanoparticles, and it reveals that the size of nanoparticles is  $<70 \text{ nm}$ . TEM image also shows some aggregated particles, which could be attributed to the TEM sample preparation process.

XRD analysis represents that the pattern of Fe<sub>3</sub>O<sub>4</sub>@Au nanoparticles coincides with reference pattern for magnetite and gold. The XRD results suggest the presence of both Fe<sub>3</sub>O<sub>4</sub> and Au crystals in the prepared sample. XRD

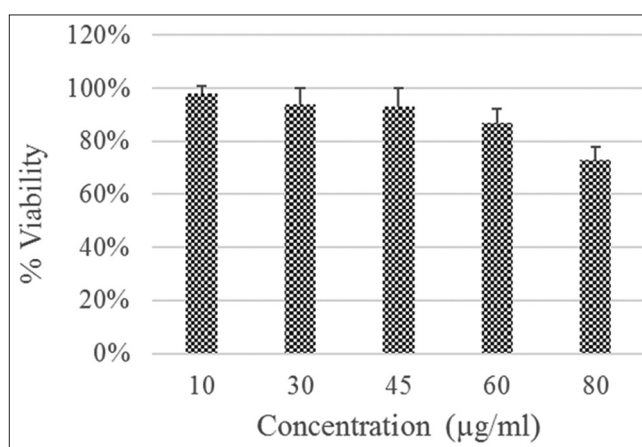


Figure 5: 3-(4,5-Dimethylthiazol-2-yl)-2,5-diphenyltetrazolium bromide assay of human hepatocellular carcinoma cells after incubation with Fe<sub>3</sub>O<sub>4</sub>@Au nanoparticles at different iron concentrations (10–80 µg/mL) after 24 h

provides information about structure and morphology of samples.

According to the FTIR spectrum, the presence of Fe<sub>3</sub>O<sub>4</sub> nanoparticles can be seen by the absorption peak at  $592 \text{ cm}^{-1}$ , which is related to the Fe–O of magnetite phase. The adsorption of SiO<sub>2</sub> layer onto the surface of Fe<sub>3</sub>O<sub>4</sub> was confirmed by bands at  $1094, 957, 804,$  and  $471 \text{ cm}^{-1}$  which were ascribed to the formation of silica shells on the surface of Fe<sub>3</sub>O<sub>4</sub>. Meanwhile, there is no absorption band for the Au in the infrared region.

According to the magnetometry result [Figure 4], it was revealed that the nanoparticles had strong magnetic responses to a changing magnetic field. Little hysteresis of nanoparticles implies that they were possess superparamagnetic properties at room temperature.<sup>[35]</sup>

MTT assay results confirmed that prepared Fe<sub>3</sub>O<sub>4</sub>@Au nanoparticles had little cytotoxicity up to  $60 \text{ µg/mL}$  and can be used safely for biomedical applications. Montazerabadi *et al.* synthesized Fe<sub>3</sub>O<sub>4</sub>@Au nanoparticles, and MTT assay showed that their nanoparticles did not have any

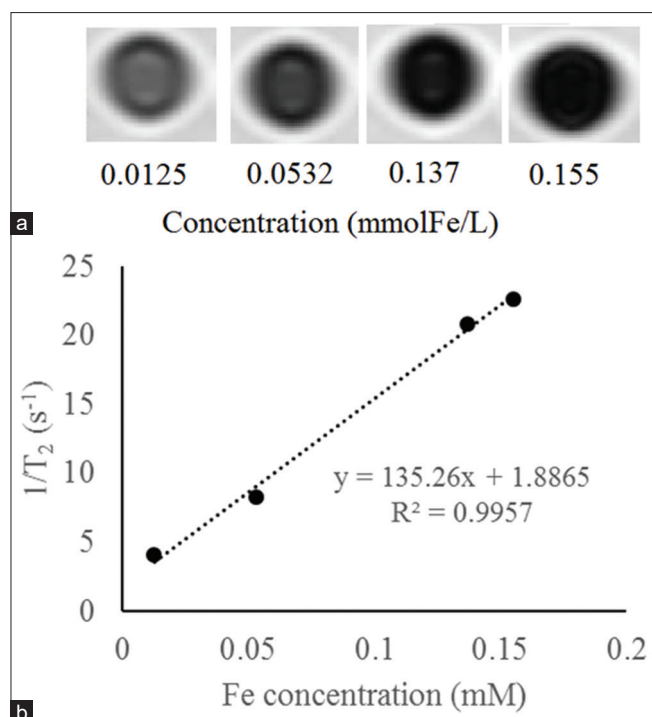


**Figure 6:** Magnetic resonance image (a) and linear fitting of transverse relaxivity rate (b) of the Fe<sub>3</sub>O<sub>4</sub>@Au nanoparticles with various Fe concentrations

cytotoxic effect on LNCaP cells.<sup>[36]</sup> The highest used Fe concentration was 115 μg/mL. Their nanoparticles showed better cytocompatibility.

Figure 6a shows that increasing in Fe concentration, decreases the signal intensity. Moreover, the MR relaxometry revealed that transverse relaxivity was 135.26 mM<sup>-1</sup>s<sup>-1</sup>. These findings confirmed the capability of synthesized Fe<sub>3</sub>O<sub>4</sub>@Au nanoparticles as an MRI contrast agent.

Figure 7 shows that as the Au concentration increases, the signal intensity increases linearly. The results were demonstrated the potential of Fe<sub>3</sub>O<sub>4</sub>@Au nanoparticles for CT imaging.

There are several preparation methods for Fe<sub>3</sub>O<sub>4</sub>/Au nanoparticles. For example, by decomposing iron pentacarbonyl on the surfaces of Au nanoparticles can prepare dumbbell-like Fe<sub>3</sub>O<sub>4</sub>/Au nanoparticles.<sup>[27]</sup> Furthermore, core/shell Fe<sub>3</sub>O<sub>4</sub>/Au nanoparticles can be prepared by synthesizing Au and thiol-functionalized nanoparticles separately and linking them by chemical bonds.<sup>[37]</sup> Another way is assembling negatively charged Au nanoparticles onto the surface of the positively charged Fe<sub>3</sub>O<sub>4</sub> nanoparticles.<sup>[38]</sup> However, in this study, magnetic iron oxide nanoparticles were prepared by co-precipitation method and then were coated with silica according to Stober method. Consequently, silica-coated nanoparticles were amino-functionalized. Finally, gold nanoparticles assembled onto the surfaces of the previous product. In this work, the synthesizing process accomplished all at

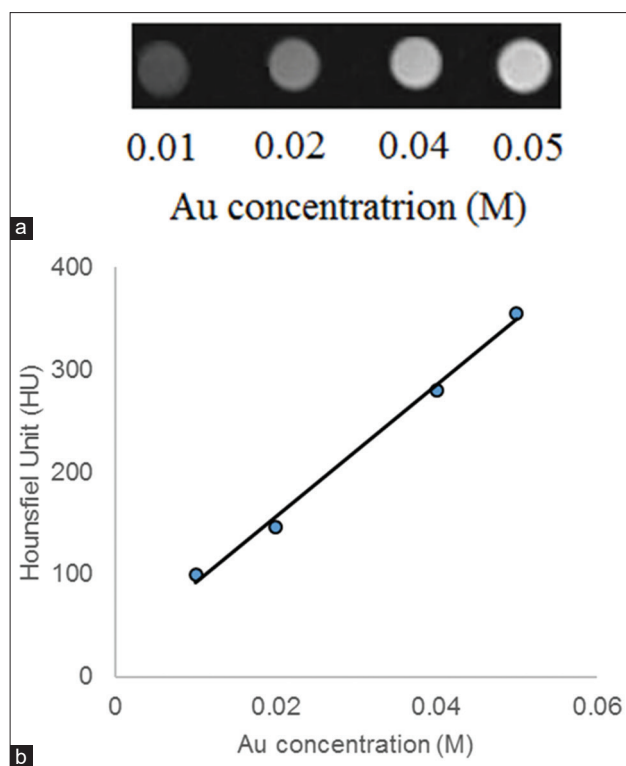


**Figure 7:** Computed tomography image of the Fe<sub>3</sub>O<sub>4</sub>@Au nanoparticles with different Au concentration (a) and X-ray attenuation of the Fe<sub>3</sub>O<sub>4</sub>@Au nanoparticles against Au concentration (b)

room temperature using convenient manner and relatively low-cost materials.

Because the main result of developing dual-modal contrast agent is to evaluate their application in imaging modalities (here, MRI and CT), their relaxivity and X-ray attenuation should be discussed. The results of the present work are in agreement with Hu *et al.*, where they synthesized hyaluronic acid-modified Fe<sub>3</sub>O<sub>4</sub>/Au nanocomposite as targeted contrast agent for CT and MRI. Their results showed that the formed nanoparticles represent a high  $r_2$  relaxivity (264.16 mM<sup>-1</sup>s<sup>-1</sup>) and good X-ray attenuation property.

Li *et al.*<sup>[39]</sup> reported synthesizing Fe<sub>3</sub>O<sub>4</sub>@Au-mPEG-PEI. NH<sub>2</sub> composite nanoparticles for dual-mode MR/CT imaging. Their results showed that nanoparticles had a relatively high  $r_2$  relaxivity of 146.07 mM<sup>-1</sup>s<sup>-1</sup> and good X-ray attenuation. The results of our study are in good agreement with Li *et al.* findings.

Cai *et al.*<sup>[40]</sup> introduced Fe<sub>3</sub>O<sub>4</sub>/Au nanocomposites by multilayer of PGA/PLL/PGA. They results showed that uncoated Fe<sub>3</sub>O<sub>4</sub>, Fe<sub>3</sub>O<sub>4</sub>@G5, and Fe<sub>3</sub>O<sub>4</sub>@Au presented  $r_2$  relaxivity of 277.81, 68.98, and 71.55 mM<sup>-1</sup>s<sup>-1</sup>, respectively. This decreasing in the value of relaxivity may be related to multilayer coating of Fe<sub>3</sub>O<sub>4</sub> nanoparticles.

In another study, Cai *et al.*<sup>[26]</sup> reported that synthesized Fe<sub>3</sub>O<sub>4</sub>/Au nanocomposites assisted by dendrimer and

using layers of poly glutamic acid and polylysine have  $r_2$  relaxivity of 92.67 mM<sup>-1</sup>s<sup>-1</sup> and good X-ray attenuation. Lower relaxivity compared to our study may be related to more layers on Fe<sub>3</sub>O<sub>4</sub> nanoparticles.

TbF<sub>3</sub> nanoparticles developed by Zheng *et al.*<sup>[19]</sup> showed a high transverse relaxivity of 395.77 mM<sup>-1</sup>s<sup>-1</sup> under 7T magnetic field. This higher relaxivity may be attributed to high magnetic field.

By considering the use of 1.5 T MRI and multicoating of Fe<sub>3</sub>O<sub>4</sub> nanoparticles in this study, our results are in good agreement with other similar researches. In addition, the findings of the present study suggested that developed Fe<sub>3</sub>O<sub>4</sub>@Au nanoparticles in easy and relatively low-cost manner can be utilized effectively in both CT and MRI applications.

## Conclusion

In summary, Fe<sub>3</sub>O<sub>4</sub>@Au nanoparticles were developed as a dual-modality MR/CT imaging contrast media. Fe<sub>3</sub>O<sub>4</sub> nanoparticles by shortening transverse relaxation time and Au nanoparticles by high X-ray attenuation property can be used for both MRI and CT, respectively. Fe<sub>3</sub>O<sub>4</sub>@Au nanoparticles showed good cytocompatibility up to 60 µg/mL, good  $r_2$  relaxivity of 135.26 mM<sup>-1</sup>s<sup>-1</sup> and a good X-ray attenuation property. It is concluded that Fe<sub>3</sub>O<sub>4</sub>@Au nanoparticles are able to be used as a contrast agent for dual-mode MR/CT imaging.

## Conflicts of interest

There are no conflicts of interest.

## References

- Thorek DL, Chen AK, Czupryna J, Tsourkas A. Superparamagnetic iron oxide nanoparticle probes for molecular imaging. *Ann Biomed Eng* 2006;34:23-38.
- Herschman HR. Molecular imaging: Looking at problems, seeing solutions. *Science* 2003;302:605-8.
- Abdolahi M, Shahbazi-Gahrouei D, Laurent S, Sermeus C, Firozian F, Allen BJ, *et al.* Synthesis and *in vitro* evaluation of MR molecular imaging probes using J591 mAb-conjugated SPIONs for specific detection of prostate cancer. *Contrast Media Mol Imaging* 2013;8:175-84.
- Zabihzadeh M, Hoseini-Ghahfarokhi M, Bayati V, Teimoori A, Ramezani Z, Assareh-zadehgan MA, *et al.* Enhancement of radio-sensitivity of colorectal cancer cells by gold nanoparticles at 18 MV energy. *Nanomed J* 2018;5:111-120.
- Jafari S, Cheki M, Tavakoli M, Zarrabi A, Sani KG, Afzalipour R. Investigation of Combination Effect Between 6 MV X Ray Radiation and Polyglycerol Coated Superparamagnetic Iron Oxide Nanoparticles on U87-MG Cancer Cells. *Journal of Biomedical Physics and Engineering*, 2018.
- Shahbazi-Gahrouei D, Abdolahi M. Superparamagnetic iron oxide-C595: Potential MR imaging contrast agents for ovarian cancer detection. *J Med Phys* 2013;38:198-204.
- Kim D, Jeong YY, Jon S. A drug-loaded aptamer-gold nanoparticle bioconjugate for combined CT imaging and therapy of prostate cancer. *ACS Nano* 2010;4:3689-96.
- Wu H, Shi H, Zhang H, Wang X, Yang Y, Yu C, *et al.* Prostate stem cell antigen antibody-conjugated multiwalled carbon nanotubes for targeted ultrasound imaging and drug delivery. *Biomaterials* 2014;35:5369-80.
- Tanaka K, Siwu ER, Minami K, Hasegawa K, Nozaki S, Kanayama Y, *et al.* Noninvasive imaging of dendrimer-type N-glycan clusters: *In vivo* dynamics dependence on oligosaccharide structure. *Angew Chem Int Ed Engl* 2010;49:8195-200.
- Zürcher NR, Bhanot A, McDougle CJ, Hooker JM. A systematic review of molecular imaging (PET and SPECT) in autism spectrum disorder: Current state and future research opportunities. *Neurosci Biobehav Rev* 2015;52:56-73.
- Hu Y, Yang J, Wei P, Li J, Ding L, Zhang G, *et al.* Facile synthesis of hyaluronic acid-modified Fe<sub>3</sub>O<sub>4</sub>/Au composite nanoparticles for targeted dual mode MR/CT imaging of tumors. *Journal of Materials Chemistry B*, 2015;3. p. 9098-9108.
- Li J, Zheng L, Cai H, Sun W, Shen M, Zhang G, *et al.* Polyethyleneimine-mediated synthesis of folic acid-targeted iron oxide nanoparticles for *in vivo* tumor MR imaging. *Biomaterials* 2013;34:8382-92.
- Shahbazi-Gahrouei D, Keshtkar M. Magnetic nanoparticles and cancer treatment. *Immunopathologia Persa* 2016;2:24.
- Biju V. Chemical modifications and bioconjugate reactions of nanomaterials for sensing, imaging, drug delivery and therapy. *Chem Soc Rev* 2014;43:744-64.
- Shahbazi-Gahrouei D, Rizvi SM, Williams MA, Allen BJ. *In vitro* studies of gadolinium-DTPA conjugated with monoclonal antibodies as cancer-specific magnetic resonance imaging contrast agents. *Australas Phys Eng Sci Med* 2002;25:31-8.
- Hainfeld JF, Smilowitz HM, O'Connor MJ, Dilmanian FA, Slatkin DN. Gold nanoparticle imaging and radiotherapy of brain tumors in mice. *Nanomedicine (Lond)* 2013;8:1601-9.
- Yong H, Jing-Chao L, Ming-Wu S, Xiang-Yang S. Formation of multifunctional Fe<sub>3</sub>O<sub>4</sub>/Au composite nanoparticles for dual-mode MR/CT imaging applications. *Chinese Physics B*, 2014;23. p. 078704-8.
- Zhou B, Xiong Z, Wang P, Peng C, Shen M, Mignani S, *et al.* Targeted tumor dual mode CT/MR imaging using multifunctional polyethylenimine-entrapped gold nanoparticles loaded with gadolinium. *Drug Deliv* 2018;25:178-86.
- Zheng X, Wang Y, Sun L, Chen N, Li L, Shi S, *et al.* TbF<sub>3</sub> nanoparticles as dual-mode contrast agents for ultrahigh field magnetic resonance imaging and X-ray computed tomography. *Nano Res* 2016;9:1135-47.
- Zheng XY, Sun LD, Zheng T, Dong H, Li Y, Wang YF, *et al.* PAA-capped GdF<sub>3</sub> nanoplates as dual-mode MRI and CT contrast agents. *Sci Bull* 2015;60:1092-100.
- Zhao HY, Liu S, He J, Pan CC, Li H, Zhou ZY, *et al.* Synthesis and application of strawberry-like Fe<sub>3</sub>O<sub>4</sub>-Au nanoparticles as CT-MR dual-modality contrast agents in accurate detection of the progressive liver disease. *Biomaterials* 2015;51:194-207.
- Wen S, Li K, Cai H, Chen Q, Shen M, Huang Y, *et al.* Multifunctional dendrimer-entrapped gold nanoparticles for dual mode CT/MR imaging applications. *Biomaterials* 2013;34:1570-80.
- Sun W, Zhang J, Zhang C, Zhou Y, Zhu J, Peng C, *et al.* A unique nanogel-based platform for enhanced dual mode tumor MR/CT imaging. *J Mater Chem B* 2018;6:4835-42.
- He X, Liu F, Liu L, Duan T, Zhang H, Wang Z. Lectin-conjugated Fe<sub>2</sub>O<sub>3</sub>@Au core@ shell nanoparticles as dual mode contrast agents for *in vivo* detection of tumor. *Mol Pharm* 2014;11:738-45.
- Chou SW, Shau YH, Wu PC, Yang YS, Shieh DB, Chen CC.

- In vitro* and *in vivo* studies of FePt nanoparticles for dual modal CT/MRI molecular imaging. *J Am Chem Soc* 2010;132:13270-8.
26. Cai H, Li K, Li J, Wen S, Chen Q, Shen M, *et al.* Dendrimer-assisted formation of Fe<sub>3</sub>O<sub>4</sub>/Au nanocomposite particles for targeted dual mode CT/MR imaging of tumors. *Small* 2015;11:4584-93.
  27. Yu H, Chen M, Rice PM, Wang SX, White RL, Sun S. Dumbbell-like bifunctional Au-Fe<sub>3</sub>O<sub>4</sub> nanoparticles. *Nano Lett* 2005;5:379-82.
  28. Beyaz S, Kockar H, Tanrisever T. Simple synthesis of superparamagnetic magnetite nanoparticles and ion effect on magnetic fluids. *Int J Optoelectronics Adv Mat Symposia* 2009;3:447-450.
  29. Stöber W, Fink A, Bohn E. Controlled growth of monodisperse silica spheres in the micron size range. *J Colloid Interface Sci* 1968;26:62-9.
  30. Chao X, Wang G, Tang Y, Dong C, Li H, Wang B, *et al.* The effects and mechanism of peiminine-induced apoptosis in human hepatocellular carcinoma HepG2 cells. *PLoS One* 2019;14:e0201864.
  31. Henoumont C, Laurent S, Vander Elst L. How to perform accurate and reliable measurements of longitudinal and transverse relaxation times of MRI contrast media in aqueous solutions. *Contrast Media Mol Imaging* 2009;4:312-21.
  32. Sillerud LO. Quantitative [Fe] MRI of PSMA-targeted SPIONs specifically discriminates among prostate tumor cell types based on their PSMA expression levels. *Int J Nanomedicine* 2016;11:357-71.
  33. Keshtkar M, Takavar A, Zahmatkesh M, Nedaie H, Vaezzadeh A, Naderi M, *et al.* Three-dimensional gel dosimetry for dose volume histogram verification in compensator-based IMRT. *Int J Radiat Res* 2014;12:13-20.
  34. Mahmoudi M, Simchi A, Milani AS, Stroeve P. Cell toxicity of superparamagnetic iron oxide nanoparticles. *J Colloid Interface Sci* 2009;336:510-8.
  35. Hong J, Xu D, Yu J, Gong P, Ma H, Yao S. Facile synthesis of polymer-enveloped ultrasmall superparamagnetic iron oxide for magnetic resonance imaging. *Nanotechnology* 2007;18:135608.
  36. Montazerabadi AR, Oghabian MA, Irajirad R, Muhammadnejad S, Ahmadvand D, Delavari H, *et al.* Development of gold-coated magnetic nanoparticles as a potential MRI contrast agent. *NANO* 2015;10:1550048-.
  37. Bao J, Chen W, Liu T, Zhu Y, Jin P, Wang L, *et al.* Bifunctional Au-Fe<sub>3</sub>O<sub>4</sub> nanoparticles for protein separation. *ACS Nano* 2007;1:293-8.
  38. Caruntu D, Cushing BL, Caruntu G, O'Connor CJ, *et al.* Attachment of gold nanograins onto colloidal magnetite nanocrystals. *Chem Mater* 2005;17:3398-402.
  39. Li J, Zheng L, Cai H, Sun W, Shen M, Zhang G. Facile one-pot synthesis of Fe<sub>3</sub>O<sub>4</sub>@Au composite nanoparticles for dual-mode MR/CT imaging applications. *ACS Appl Mater Interfaces* 2013;5:10357-66.
  40. Cai H, Li K, Shen M, Wen S, Luo Y, Peng C, *et al.* Facile assembly of Fe<sub>3</sub>O<sub>4</sub>@Au nanocomposite particles for dual mode magnetic resonance and computed tomography imaging applications. *J Mater Chem* 2012;22:15110-20.

## BIOGRAPHIES



**Mohammad Keshtkar** is an assistant professor of Medical Physics at the Department of Medical Physics and Radiology, Gonabad University of Medical Sciences, Gonabad, Iran. He received his B.Sc. in Radiology Technology from School of Paramedical Sciences, Shiraz University of Medical Sciences, Shiraz, Iran, M.Sc. degree

in Medical Physics from Tehran University of Medical Sciences, Tehran, Iran and Ph.D. in Medical Physics from Isfahan University of Medical Sciences, Isfahan, Iran.

**Email:** keshtkar.dmohammad@yahoo.com



**Daryoush Shahbazi-Gahrouei** is a Professor of Medical Physics at the Isfahan University of Medical Sciences, Isfahan, Iran. He received his B.Sc. in Physics from School of Science, Isfahan University, Iran, M.Sc. degree in Medical Physics from Tarbiat Modarres University, Tehran, Iran, and Ph.D. in Medical Physics from University of

Western Sydney and St. George Cancer Care Centre, Sydney, Australia.

**Email:** shahbazi@med.mui.ac.ir



**Alireza Mahmoudabadi** is an assistant professor of Radiology at the at the Department of Medical Physics and Radiology, Gonabad University of Medical Sciences, Gonabad, Iran. He received his MD degree from School of Medicine, Mashhad University of Medical Sciences, Mashhad and Radiology from School of

Medicine, Mashhad University of Medical Sciences, Mashhad, Iran.

**Email:** Mahmoudabadi\_md@yahoo.com